Journal of Hydrology 516 (2014) 97–106

Contents lists available at ScienceDirect

Journal of Hydrology

journal homepage: www.elsevier.com/locate/jhydrol

The role of macropores and multi-resolution soil survey datasets for distributed surface–subsurface flow modeling

Xuan Yu [a], Christopher Duffy [a,*], Doug C. Baldwin [b], Henry Lin [c]

[a] Department of Civil and Environmental Engineering, The Pennsylvania State University, University Park, PA 16802, USA
[b] Department of Geography, The Pennsylvania State University, University Park, PA 16802, USA
[c] Department of Ecosystem Science and Management, The Pennsylvania State University, University Park, PA 16802, USA

ARTICLE INFO

Article history:
Available online 3 March 2014

Keywords:
PIHM
Macropore
Subsurface storm flow
Shale Hills
CZO
Soil survey

SUMMARY

Distributed watershed-scale modeling is often used as a framework for exploring the heterogeneity of runoff response and hydrologic performance of the catchment. The objective of this study is to apply this framework to characterizing the impacts of soil hydraulic properties at multiple scales on moisture storage and distributed runoff generation in a forested catchment. The physics-based and fully-coupled Penn State Integrated Hydrologic Model (PIHM) is employed to test a priori and field-measured properties in the modeling of watershed hydrology. PIHM includes an approximate representation of macropore flow that preserves the water holding capacity of the soil matrix while still allowing rapid flow through the macroporous soil under wet conditions. Both phenomena are critical to the overall hydrologic performance of the catchment. Soils data at different scales were identified: Case I STATSGO soils data (uniform or single soil type), Case II STATSGO soils data with macropore effect, and Case III field-based hydropedologic experiment revised distributed soil hydraulic properties and macropore property estimation. Our results showed that the Case I had difficulties in simulating the timing and peakflow of the runoff responses. Case II performed satisfactorily for peakflow at the outlet and internal weir locations. The distributed soils data in Case III demonstrated the model ability of predicting groundwater levels. The analysis suggests the important role of macropore flow to setting the threshold for recharge and runoff response, while still preserving the water holding capability of the soil and plant water availability. The spatial variability in soil hydraulic properties represented by Case III introduces an additional improvement in distributed catchment flow modeling, especially as it relates to subsurface lateral flow. Comparison of the three cases suggests the value of high-resolution soil survey mapping combined with a macropore parameterization can improve distributed watershed models.

1. Introduction

Subsurface lateral flow has been widely recognized as important to the generation of stormwater runoff (Alaoui et al., 2011; McGuire and McDonnell, 2010; Tromp-van Meerveld and McDonnell, 2006a,b), to the study of preferential flow (Thomas et al., 2013; Graham and Lin, 2011; Lin, 2010; Vogel et al., 2010), and to the evaluation of nutrient fluxes (Dhillon and Inamdar, 2013; Hwang et al., 2012; Zhang et al., 2011). However, direct observation of the occurrence and distribution of subsurface lateral flow at the hillslope scale has been constrained by temporal dynamics and spatial heterogeneity. To gain an improved conceptual understanding, mathematical models for vadose zone hydrology were developed to explore the hillslope scale hydrological processes (Hopp and McDonnell, 2009; Kabat et al., 1997; Lehmann et al., 2007; Mirus and Loague, 2013).

The issue related to upscaling measured hydraulic parameters from use in catchment scale modeling applications are being tested more frequently than ever, mostly because of the capability of integrated environment models in the understanding of water resources and quality in subsurface and surface water systems. Early modeling applications proved that the effective soil hydraulic parameters could adequately describe the lumped hydrological behavior (Feddes et al., 1993; Kabat et al., 1997). However, the effective soil hydraulic parameters for modeling studies are difficult to obtain from aggregation of soil types (Kabat et al., 1997). Only a few studies have reported the effects of soil spatial variability on hydrological response to input resolution of spatial data. Mirus et al. (2011) argued that reducing the representation of spatially variability of soil hydraulic properties did not affect the dominant runoff generation processes, and the reduced spatial

* Corresponding author. Tel.: +1 814 863 4384; fax: +1 814 863 7304.
E-mail address: cxd11@psu.edu (C. Duffy).

http://dx.doi.org/10.1016/j.jhydrol.2014.02.055
0022-1694/

complexity could still retain the ability to simulate the overall hydrograph and runoff pattern. This conclusion raises the question of the resolution of soil hydraulic properties for watershed modeling.

Another important issue for distributed catchment modeling is the representation of preferential flow. In forested catchments, preferential flow through macropores such as root holes, cracks or pipes in soils, or through dissolutions features, joints, and fractures in bedrock can lead to large and fast infiltration and recharge to groundwater (Aubertin, 1971; Anderson et al., 1997). Even though the macroporous volume is small relative to the soil matrix, the volumetric transport capacity can be significant to the overall flow (Watson and Luxmoore, 1986). The critical pore size at which infiltration can be classified as macropore flow has been discussed in Beven and Germann (1982). Several studies have focused on approximating the macropore flow contributions to subsurface flow (Hutson and Wagenet, 1975; Gerke and van Genuchten, 1993; Mohanty et al., 1997; Vanderkwaak, 1999). It has been found that modeling with a macropore flow concept yields improvements than without macropores (Tromp-van Meerveld and Weiler, 2008; Van Schaik et al., 2010; Beven and Germann, 2013).

This study compares the effects of multi-resolution soil data from national databases, and in situ field observations on the overall hydrologic performance of the Shale Hills Catchment. According to State Soil Geographic (STATSGO) Data uniform soil type is applied at Shale Hills Catchment. To obtain higher resolution soil information we used the results of Baldwin (2011). In the experiment, catchment-wide maps of saturated moisture content, depth to bedrock, and slope value were used to delineate map units with similar soil moisture patterns. The multi-resolution soils data led to three model scenarios: Case I: STATSGO data without macropore effect; Case II: STATSGO data adding macropore effect; and Case III: hydropedologic functional units data with macropore effect. This study employed a fully coupled physics-based integrated model: Penn State Integrated Hydrologic Model (PIHM) to evaluate the effects of spatial soil pattern on subsurface flow and overall catchment model performance.

2. Materials and methods

2.1. Site description

The Shale Hills site that we used to test the soil hydraulic properties spatial pattern is a 0.08-km^2 forested watershed managed by the Pennsylvania State University. A program of research using Earth's Critical Zone Observatories (CZOs) has been initiated, and Shale Hills is one the CZOs: the Susquehanna-Shale Hills Critical Zone Observatory (SSHCZO), which focuses on hydrologic flow paths and timescales, as well as the regolith formation, ecosystem dynamics within a small, forested catchment. To date, intensive observed environmental variables have been examined to identify the prominence of hydrologic processes including soil moisture dynamics (Lin and Zhou, 2008; Lin, 2006), subsurface flow pathways (Thomas et al., 2013; Graham and Lin, 2011; Zhang, 2011; Zhang et al., 2014), solute transport (Andrews et al., 2011; Jin et al., 2010; Kuntz et al., 2011), and stream flow generation mechanisms (Lynch, 1976; Lynch and Corbett, 1985). Using field studies as a basis, modeling studies have reported on the antecedent moisture impacted peak flow generation (Qu and Duffy, 2007), land surface energy balance (Shi et al., 2013).

The watershed is situated in the Ridge-and-Valley Appalachians in the Central Pennsylvania (Fig. 1). The climate in Central Pennsylvania represents a humid continental climate. Extreme temperatures have been recorded 39 °C and −29 °C. Precipitation is relatively seasonally uniform. As an experiment site, extensive data sets were examined including topography, soil moisture sampling, soil mapping, streamflow, subsurface flow, and stand characteristics (Baldwin, 2011; Lin, 2006; Meinzer et al., 2013; Zhang, 2011).

The watershed overlies continuous Rose-Hill Shale bedrock with the strike and dip of N54°E and 76°NW (Jin et al., 2010). The bedrock has been set as a no-flow boundary of near surface hydrologic modeling (Qu and Duffy, 2007). The thickness of the soil layer ranges from <0.25 m on the ridge tops and upper side slopes to >2 m in the valley bottom and swales (Lin et al., 2006). Based on field measurements, lateral subsurface flow has been identified as a dynamic part in the watershed hydrologic cycle (Graham and Lin, 2011; Lin et al., 2006). In situ soil moisture measurement suggested that preferential flow is very common in the watershed (Lin and Zhou, 2008). The solute transport tests demonstrated that the preferential flow path is a significant factor controlling transport behavior at the watershed (Kuntz et al., 2011).

The vegetation cover of Shale Hills is a mixture of deciduous forest and evergreen forest. Major species include *Quercus prinus*, *Quercus rubra*, *Quercus alba*, *Tsuga canadensis*, *Carya tormentosa*, *Acer saccharum*, *Carys glabra*, *Pinus sstrobus*, *Pinus virginiana* (Meinzer et al., 2013; Naithani et al., 2013). The rooting zone is extremely shallow, and the majority of the roots are situated in the organic horizon and eluvial horizon (Meinzer et al., 2013; Lin, 2006).

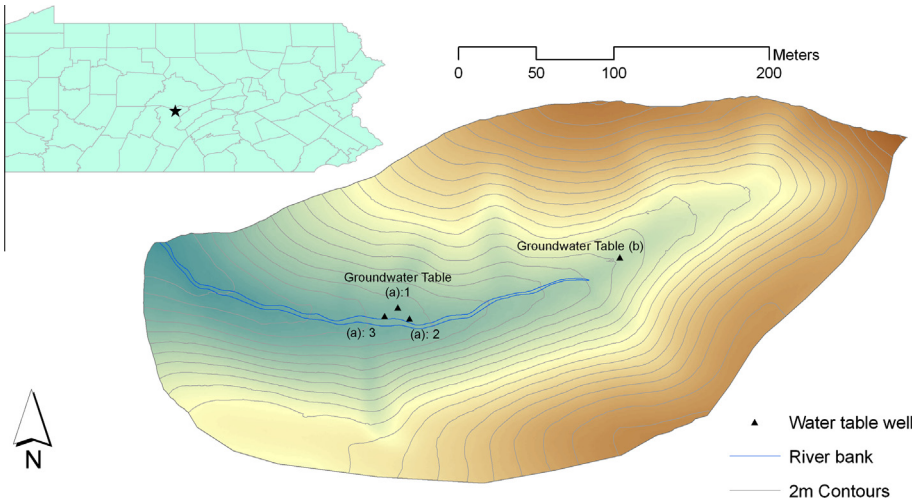

Fig. 1. Location of the Shale Hills Catchment in Pennsylvania.

2.2. Representation of soil hydrological properties

Up to now, three sets of soils data have been developed (Table 1 and Fig. 2):

(1) The State Soil Geographic database (STATSGO) (USDA NRCS).
(2) Order I precision soil map (Lin et al., 2006).
(3) Hydropedologic functional units (HFUs) (Baldwin, 2011).

Each of these three soils datasets is briefly described in the following. Related details can be found in Lin et al. (2006) and Baldwin (2011).

(1) In the STATSGO, the SSHCZO catchment is entirely mapped as Weikert–Berks soil series combination (Fig. 2). This uniform soil type is generally shallow and well-drained. Qu and Duffy (2007) applied the hydrological properties of Weikert–Berks (Table 1) in PIHM throughout the whole watershed, and the model results explained the effect of antecedent soil moisture on the runoff peak and timing.
(2) The Order I soil survey at the SSHCZO has produced a precision soil map that improved spatial soil heterogeneity by distinguishing a total of five soil series: Weikert, Berks, Rushtown, Blairton, and Ernest (Lin et al., 2006). Soil hydraulic properties for each of these five soil series have been characterized (Table 1).
(3) Based on the precision soil map, together with LIDAR topography, soil moisture storage monitoring data, and soil water retention curves, Baldwin (2011) has developed a hydropedologic functional units (HFUs) system for the SSHZO, in which he identified five HFUs: Deep Soil, High Storage, Flat Valley (DSHSFV); Deep Soil, High Storage, Concave Hillslope (DSHSCH); Intermediate Soil, Medium Storage, Convex Hillslope (ISMSCH); Shallow Soil, Low Storage, Planar Hillslope (SSLSPH); and Shallow Soil, Low Storage, Flat Summit (SSLSFS). These HFUs provide an improved spatial mapping of soil hydraulic properties for distributed hydrologic modeling. To delineate HFUs, three hillslope map units with different moisture storage and soil depths were generated first. A principal component analysis was conducted on the catchment-wide saturated soil moisture and depth to bedrock maps, and the loadings at each grid cell from the principal component analysis (PCA) analysis were then inputted into a c-means clustering algorithm with three clusters specified. The PCA was essential for reducing multi-collinearity between saturated soil moisture and depth to bedrock data. After the hillslope units were defined, a slope map was used to define flat areas in the deep, high-storage hillslope unit and the shallow, low-storage hillslope unit. These flat areas became separate valley and summit units, which generated a total of five HFUs in the Shale Hills.

2.3. Description of the hydrologic model

PIHM is a physics-based, fully coupled, spatially distributed, hydrologic model. It simulates the terrestrial water cycle including interception, throughfall, infiltration, recharge, evapotranspiration, overland flow, unsaturated soil water, groundwater flow, and channel routing, in a fully coupled scheme (Qu and Duffy, 2007). Evapotranspiration is calculated using the Penman–Monteith approach adapted from Noah_LSM (Chen and Dudhia, 2001). Overland flow is described in 2-D estimated of St. Venant equations. Movement of moisture in unsaturated zones is assumed to be vertical, which is modeled using Richard's equation. The model assumes that each subsurface layer can have both unsaturated and saturated storage components. The recharge to and from the water table couples the unsaturated and saturated zones. The channel routing is modeled using 1-D estimation of St. Venant equations. We use diffusive wave approximation for channel routing and overland flow. For saturated groundwater flow, the 2-D Dupuit approximation is applied (Qu and Duffy, 2007). Spatially, the modeling domain is decomposed into Delaunay triangles. The unstructured mesh allows users to resolve spatial data over the watershed. The triangular mesh can be constrained by point or vector data (e.g., stream gauge, wells, soil maps, and land cover), and the watershed boundary conditions (Kumar, 2009). The model resolves hydrological processes for land surface energy, overland flow, channel routing, and subsurface flow, governed by partial differential equation (PDE) system. The system is discretized on the triangular mesh and projected prism from canopy to bedrock. PIHM uses a semi-discrete finite-volume formulation for solving the system of coupled PDEs, resulting in a system of ordinary differential equations (ODE) representing all processes within the prismatic control volume. Here we gave a brief illustration of the model coupling strategy in Fig. 3, and Table 2. Detailed descriptions of the rest of modeling theory and the full set of mathematical formulation can be found at the PIHM website (http://www.pihm.psu.edu/) and associated publication (Kumar, 2009; Qu and Duffy, 2007).

Table 1
Soil units and their basic texture and hydraulic parameters at different scales (see Fig. 2 for soil spatial distribution).

Data source	Soil series (units)	Texture			Soil hydraulic parameters				
		Sand (%)	Silt (%)	Clay (%)	θs	θr	Air-entry suction α (m^{-1})	Pore size distribution β	Ks (m/day)
STATSG*	Weikert–Berks	27–34	47–58	15–19	0.4	0.05	2	1.8	0.864
Order I soil survey**	Weikert	32	45	23	0.64	0.0653	2.46	1.59	40.32
	Berks	43	36	21	0.37	0.0556	2.51	1.71	2.68
	Rushtown	50	31	18	0.38	0.0556	2.84	1.71	4.25
	Blairton	47	33	20	0.37	0.0556	2.79	1.71	9.36
	Ernest	39	45	16	0.37	0.0556	2.56	1.71	2.68
Hydropedologic functional units***	Deep Soil, High Storage, Flat Valley (DSHSFV)	32	45	23	0.43	0.062	10.8	1.22	N/A
	Deep Soil, High Storage, Concave Hillslope (DSHSCH)	47	37	16	0.35	0.062	10.4	1.27	N/A
	Intermediate Soil, Medium Storage, Convex Hillslope (ISMSCH)	46	41	14	0.28	0.049	8.4	1.28	N/A
	Shallow Soil, Low Storage, Planar Hillslope (SSLSPH)	47	37	16	0.24	0.029	11.7	1.25	N/A
	Shallow Soil, Low Storage, Flat Summit (SSLSFS)	43	36	20	0.24	0.027	10.5	1.21	N/A

* Data were retrieved from http://www.soilinfo.psu.edu/ and Qu and Duffy (2007).
** Data were retrieved from Lin (2006).
*** Data were retrieved from Baldwin (2011).

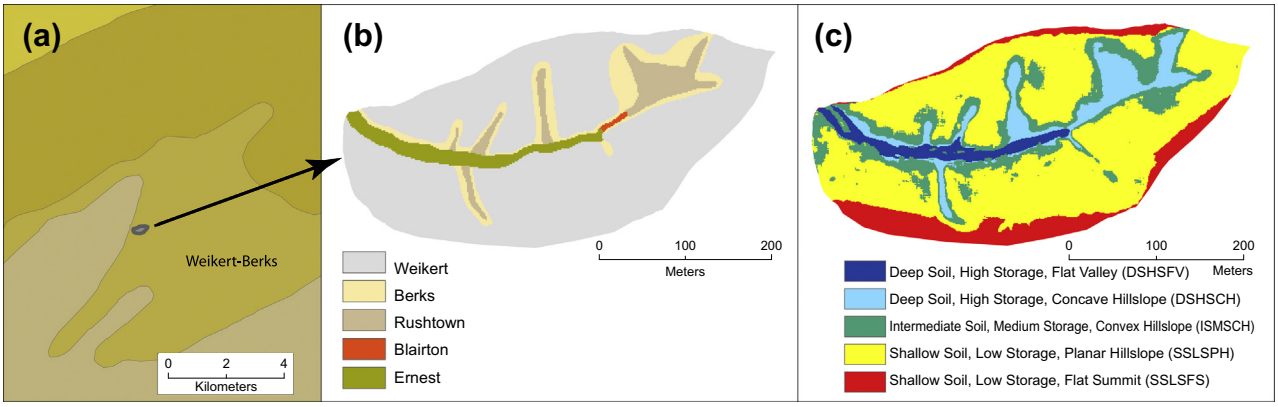

Fig. 2. Comparison of the three soil data sets at Shale Hills Catchment: STATSGO (left column), Order I soil survey map (Lin, 2006) (middle column), and hydropedologic functional units (Baldwin, 2011) (right column).

We follow a simple approximation to the dual-domain approach that uses a weighted piecewise-continuous hydraulic function of soil water retention and hydraulic conductivity function by weighting the coarse and fine pore fractions for the Shale Hills Catchment (Duffy et al., 2000; Mohanty et al., 1997). The approach represents an equivalent matrix–macropore dual system that is assumed to follow Richard's equation with total infiltration/exfiltration rate to be equal to sum of matrix infiltration and macropore infiltration. In addition to the increase in soil infiltration capacity, a second effect of a macroporous soil is the possible lateral conduction of subsurface stormflow (Mosley, 1982). The macropore system (as defined here) also results in quick transmission of soil water as subsurface stormflow or interflow. The depth of this interflow layer is assumed to be the depth of the macroporous soil, which will depend on the vegetation type and root distribution, organic content and geologic materials. The piecewise-continuous approach outlined was implemented in the PIHM model (see Kumar, 2009). Specifically, we take macropore effect into account when we calculate the infiltration conductivity (Rawls et al., 1993) and lateral subsurface flow conductivity. The effective hydraulic conductivity (K_{eff}) is defined as a porosity-weighted average of the matrix conductivity (K_{MX}) and macropore conductivity (K_{MP}):

$$K_{eff}(\Psi) = K_{MX}(\Psi) \cdot (1-\beta) + K_{MP}(\Psi) \cdot \beta$$

where β is the fraction of the total porosity that is composed of macropores (Chen and Wagenet, 1992). The macropore conductivity (K_{MP}) is estimated as the product of the saturated-hydraulic conductivity and a macroporosity factor (Rawls et al., 1993).

The model domain is interpreted in Fig. 3. We used 535 triangles to represent the landform heterogeneity of the SSHCZO. The average area of the triangles was 157.3 m^2. We used 20 linear segments to represent the rectangular shape stream channel, and the average length was 15.0 m.

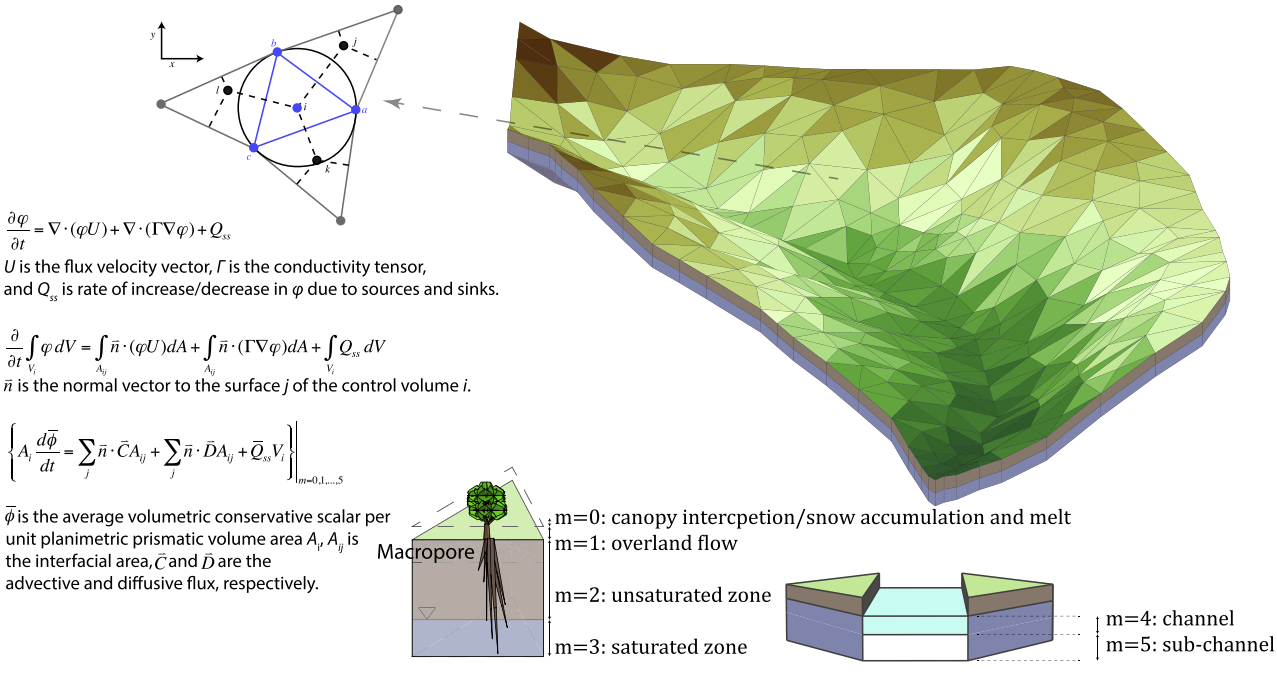

Fig. 3. The PIHM representation of hydrological processes and model coupling strategy. The triangle mesh represents the spatial domain decomposition. The equations demonstrate semidiscrete finite volume formulation for each computational grid. The equations are applied on each process, and then assembled over the whole domain. Related details can be found in Qu and Duffy (2007) and Kumar (2009).

Table 2
Main equations of PIHM.

Process	Governing equation/model	Original governing equations	Semi-discrete form*
Interception	Bucket model	$\frac{dh}{dt} = P - E_c - P_t$	$\left(\frac{dh_{0I}}{dt} = P - E_c - P_t\right)_i$
Snowmelt	Temperature index model	$\frac{dh}{dt} = P - E_{snow} - \Delta w$	$\left(\frac{dh_{0S}}{dt} = P - E_{snow} - \Delta w\right)_i$
Evapotranspiration	Penman–Monteith approach	$ET_0 = \frac{\Delta(R_n - G) + \rho_a C_p \frac{(\varepsilon_s - \varepsilon_a)}{r_a}}{\Delta + \gamma\left(1 + \frac{r_s}{r_a}\right)}$	$\left(ET_0 = \frac{\Delta(R_n - G) + \rho_a C_p \frac{(\varepsilon_s - \varepsilon_a)}{r_a}}{\Delta + \gamma\left(1 + \frac{r_s}{r_a}\right)}\right)_i$
Overland flow	St. Venant equation	$\frac{\partial h}{\partial t} + \frac{\partial (uh)}{\partial x} + \frac{\partial (vh)}{\partial y} = q$	$\left(\frac{dh_1}{dt} = p_n - q^+ - e + \sum_{j=1}^{3} q_j^s\right)_i$
Unsaturated flow	Richard equation	$C(\Psi)\frac{\partial \Psi}{\partial t} = \nabla \cdot (K(\Psi)\nabla(\Psi + Z))$	$\left(\theta_s \frac{dh_2}{dt} = q^+ - q^0\right)_i$
Groundwater flow			$\left(\theta_s \frac{dh_3}{dt} = q^0 + \sum_{j=1}^{3} q_j^g\right)_i$
Channel flow	St. Venant equation	$\frac{\partial h}{\partial t} + \frac{\partial (uh)}{\partial x} = q$	$\left(\frac{dh_{4,5}}{dt} = p - e + \sum_{j=1}^{2}(q_l^s + q_l^g) + q_{in}^c - q_{out}^c\right)_k$

* *Notation:* h_{0I} is the vegetation interception storage, P is the precipitation, E_c is the evaporation from canopy interception, p_t is the throughfall. h_{0S} is the snow water equivalent storage, E_{snow} is the snow sublimation rate, Δw is snow-melting rate. Δ is the slope of the saturation vapor pressure–temperature relationship, R_n is net radiation at the vegetation surface, G is soil heat flux density, $\varepsilon_s - \varepsilon_a$ represents the air vapor pressure deficit, and ρ_a is the air density, C_p is specific heat of the air, γ is the psychometric constant, r_s and r_a are the surface and aerodynamic resistances. h_1 is the shallow water depth above the ground surface, p_n, q^+ and e are the net precipitation, infiltration, and evaporation, respectively, q_j^s is the normalized lateral flow rate from element i to its neighbor j. θ_s is the moisture content, h_2 is the unsaturated storage depth, h_3 is the groundwater depth, q^0 is flux between unsaturated–saturated zone, q_j^g is the normalized lateral groundwater flow rate from element i to its neighbor j. $h_{4,5}$ is depth of water in the channel or beneath the channel, q_l^s and q_l^g are the lateral surface flow and groundwater interaction with the channel respectively from each side of the channel or beneath the channel, the upstream and downstream flow for each channel segment or beneath the channel are q_{in}^c and q_{out}^c respectively. Subscript i represents the spatial grid, and subscript k represents the channel segment.

2.4. Experiment design

Spatial heterogeneity of subsurface flow is rarely modeled and validated due to the difficulty to validate with observed data. Here, we used a spatially distributed model and high-resolution data to test the mechanism of lateral subsurface flow in runoff generation. The national scale soil data was revised at catchment scale with field data (Order I soil survey and HFUs). We evaluated the impact of soil data scale in the fully coupled physics-based model: PIHM. Specifically, we used the coarse soil data (STATSGO data) and latest revised data (HFUs), combined with macropores effects, and then set model simulation cases: Case I used uniform (or single) soil type of hydraulic parameters from STATSGO, Case II added the macropore effect (controlled by macropore hydraulic conductivities and macroporosity percentages laterally and vertically, 1% was assumed as default value), and Case III applied HFU soil hydraulic parameters with both spatial variation and macropore effect. We compared the model results from the three cases with respect to runoff, saturated storage. The differences were used to reveal the runoff generation mechanisms, and to confirm the role of macropore effects and distributed soil properties in catchment scale hydrological processes.

2.5. Model calibration

The calibration of PIHM usually involves the optimization of saturated hydraulic conductivity, saturated water content, residual water content, soil hydraulic parameters for the van Genuchten model (van Genuchten, 1980), the area proportion of soil macroporosity, vegetation fraction, field capacity, wilting point, maximum interception storage capacity factor, and minimum canopy resistance. Yu et al. (2013) partitioned these parameters into event-scale group (sensitive to hydrologic events) and seasonal time scale group (sensitive to seasonal changes in the energy balance). In this study, we focused on event-scale hydrological responses. Therefore, we did the calibration on the event-scale group parameters (Table 3). In the calibration, we optimize the objective f: $\mathbf{R}^n \rightarrow R$, where the n is the dimension of the problem.

The objective f was the metric of outlet runoff. $\mathbf{R}^n$ included the single group of soil hydraulic parameters from STATSGO.

$$f = 1 - NSE_{streamflow}$$

where $NSE_{streamflow}$ is the Nash–Sutcliffe efficiency coefficient of streamflow. $\mathbf{R}^n$ was the set of scale factors of soil hydraulic properties and channel parameters (Table 3). In Case I, parameters of macropore were set as zero to disable macropore effect. The parameter optimization used the Covariance Matrix Adaptation Evolution Strategy (Hansen, 2011) to select the best parameters for PIHM (Yu et al., 2013).

3. Results

For each case the model was calibrated using the method outlined in Yu et al. (2013). The calibrated optimal values of soil hydraulic parameters are listed in Table 4. In the Case I without macropores, the calibration results showed increased conductivity, increased saturated water content, reduced α and increased β comparing with the priori parameters from STATSGO database (Table 1). In the Case II, we employed macropore effect, and the macropore effect reached as deep as 2.06 m. The macropores

Table 3
Selected parameters used in the PIHM for calibration.

Parameter	Hydrological processes	Priori estimation	Range
Matrix conductivity	Subsurface flow	Pedotransfer functions* from soil texture; field data**	2 order (multiply by 0.01–100)
Macropore conductivity	Subsurface flow	100 times of matrix conductivity*	2 order (multiply by 0.01–100)
Topsoil conductivity	Infiltration	Pedotransfer functions* from topsoil texture; field data	2 order (multiply by 0.01–100)
Macropore depth	Subsurface flow	Estimated from root system	0–bedrock depth
Porosity	Subsurface flow	Pedotransfer functions* from soil texture; field data**	0–1
Air-entry suction α	Subsurface flow, recharge	Pedotransfer functions* from soil texture	1 order (multiply by 0.1–10)
Pore size distribution β	Subsurface flow, recharge	Pedotransfer functions* from soil texture	1 order (multiply by 0.1–10)
River bed conductivity	Channel routing	Hard coded to be 1.0 (vertical) and 0.1 lateral m/day**	2 order (multiply by 0.01–100)
River Manning's roughness	Channel routing	Dingman (2002)	1 order (multiply by 0.1–10)

* The pedotransfer functions are from Wösten et al. (2001).
** Parameters have both vertical and lateral values.

increased the hydraulic conductivity as much as 10–100 times. In the Case III, the soil heterogeneity was reflected in the variation of parameters for the five types. To understand role of soil hydraulic parameters, we compared the PIHM results on runoff, saturated storage.

3.1. Runoff

The Case I generated a poor prediction of the runoff at the outlet (Fig. 4). The storm could not reach at the outlet immediately after the rainfall events. As a result of macropore effect above a threshold depth (macropore depth), the model reproduced the nonlinear runoff response in Cases II and III (Fig. 4). The modeled responses of internal runoff showed significant difference due to the macropore effects. Case I (without macropore effects) had longer lag time and less volume of peakflow, and flatter rising and falling limb in the hydrograph comparing with Case II and Case III (with macropore effects), which turned to be more obvious in the internal runoff at weir 2, 3, and 4 (Fig. 4). The hydrographic behavior in Cases II and III are similar due to the macropore effect representation in the model. The difference of drainage characteristics of single versus dual continuum soil was proved by core scale modeling scenarios (Vogel et al., 2000). The result suggested that the drainage of water from the bottom of the profile occurred significantly earlier for dual- than for single-permeability scenarios. Similarly, our watershed scale modeling of Case II and Case III (with macropore effects) showed rapid decline of streamflow than that of Case I (without macropore effects) during the flow recession.

3.2. Saturated storage

The water table dynamics at four groundwater wells were plotted in Fig. 5. The water table depth (in Fig. 5a) was the mean of three wells located at each node in the triangle mesh element (Fig. 1). Another groundwater well was located at upslope. Clearly Case III with soil heterogeneity demonstrated the ability to capture the water table dynamics at both sites in different soil types. While in Cases I and II, the model results failed to capture the water table dynamics.

The spatial water table dynamics were examined at different time during the storm (A–E, Fig. 6). We used the pre-storm condition (A) as the initial reference, and then plot the water table variation at B (peak flow reached), C (at the beginning of recession), D (in the middle of recession), E (after recession) (Fig. 7). In all the cases, the water table elevation follows landform topography. In Case I, the water table suggested a considerable height of rising to produce large volume of stormflow. The simulated water table difference between A and B showed considerable increase at upslope and slight increase near the stream. The exaggerated water table difference between upslope and downslope resulted high hydraulic gradient to produce stormflow. In Cases II and III, the macropore effect was employed. The water table dynamic followed landform topography and spatial soil pattern. Case II employed uniform soil parameters, and the rising and falling pattern of water table happened mainly near the stream. The heterogeneity of soil in Case III resulted different water table dynamics following the HFU pattern. We plotted the lumped behavior of saturated storage. The average percentage change in saturated storage relative to the total pore volume is illustrated in Fig. 8. In Case I, the watershed was more than half-saturated to produce the immediate stormflow response. While, in Cases II and III, the precipitation could rapidly infiltrated into subsurface and discharged into stream channel, therefore the whole processes did not result in dramatic variation in the saturated storage.

4. Discussion

Previous work at the SSHCZO has identified the flow or transport processes in the catchment at different scales (Lin, 2006; Lin and Zhou, 2008; Graham and Lin, 2011). Vertical preferential flow has been identified as occurring due to various macropores, hydrophobicity, and high contrast permeability soils, while lateral preferential flow occurs along lateral macropores and soil horizon and/or soil–bedrock interfaces (Lin and Zhou, 2008; Graham and Lin, 2011). Our modeling results in this study support these observations and provide further insight into watershed-scale hydrologic processes, as elaborated in the following.

4.1. Subsurface flow and macropore effect

Field studies have reported substantial macropore subsurface flow at SSHCZO. Lin et al. (2006) identified lateral macropore flow at A–B horizon interface from spatial soil moisture monitoring results. The lateral flow pathway is one of the major contributions of immediate streamflow response to the precipitation. To explained the mechanism of subsurface flow triggered storm events, literature uses "precipitation threshold" to identify the subsurface stormflow (Dunne, 1978; Lehmann et al., 2007; Lin and Zhou, 2008; Tromp-van Meerveld and McDonnell, 2006b; Weiler and McDonnell, 2004). Tromp-van Meerveld and McDonnell (2006a) found that a threshold of 55 mm of precipitation could distinguish the subsurface stormflow of 2 orders magnitude difference. And then, "fill and spill mechanism" was employed to describe the process of subsurface saturation before significant subsurface flow can occur (Tromp-van Meerveld and McDonnell, 2006b). It well explained that when storm total precipitation is larger than 55 mm, the water level in the bedrock depression rises high enough that water spills downslope over the bedrock ridge. Similarly, the threshold-like hillslope hydrologic response was found at SSHCZO. Lin and Zhou (2008) claimed that the rainfall intensity of 2 mm per 10 min could be the possible threshold for SSHCZO. However the six equal artificial rainfall events in 1974 generated significant

Table 4
Calibrated soil parameters and their optimal values for the PIHM simulations.

	Soil Series	θs	θr	van Genuchten model parameters		Saturated K of matrix		Saturated K of macropore		Macropore depth (m)
				Air-entry suction α (m^{-1})	Pore size distribution β	Horizontal (m/day)	Vertical (m/day)	Horizontal (m/day)	Vertical (m/day)	
Case I	Weikert–Berks	0.51	0.05	1.045	6.73	70.29	5.03	N/A	N/A	N/A
Case II	Weikert–Berks	0.40	0.05	1.40	2.75	15.36	0.38	113.79	86.16	2.06
Case III	DSHSFV	0.59	0.062	1.36	2.81	38.42	0.21	715.21	2.58	1.76
	DSHSCH	0.48	0.062	1.31	2.92	5.39	0.59	481.32	14.5	2.11
	ISMSCH	0.39	0.049	1.06	2.94	7.21	0.79	36.74	50.76	0.60
	SSLSPH	0.33	0.029	1.48	2.88	5.34	0.51	491.21	44.21	2.20
	SSLSFS	0.33	0.027	1.33	2.78	4.90	0.21	45.27	14.95	1.50

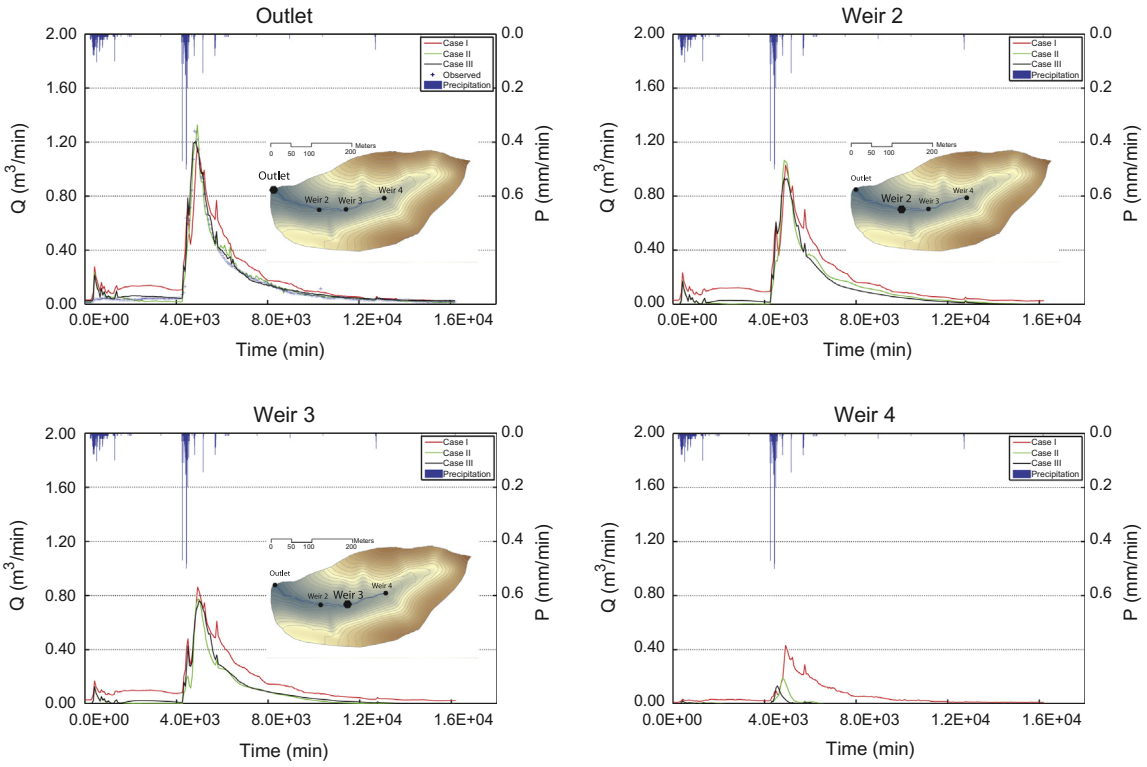

Fig. 4. Modeled runoff for the event in 2009 (from June 17th to June 28th). Note that Case I (red) had difficulties to reproduce the quick stream flow responses. Case II (green) and Case III (black) had similar results in both outlet runoff and internal runoff (weir 2–4). (For interpretation of the references to color in this figure legend, the reader is referred to the web version of this article.)

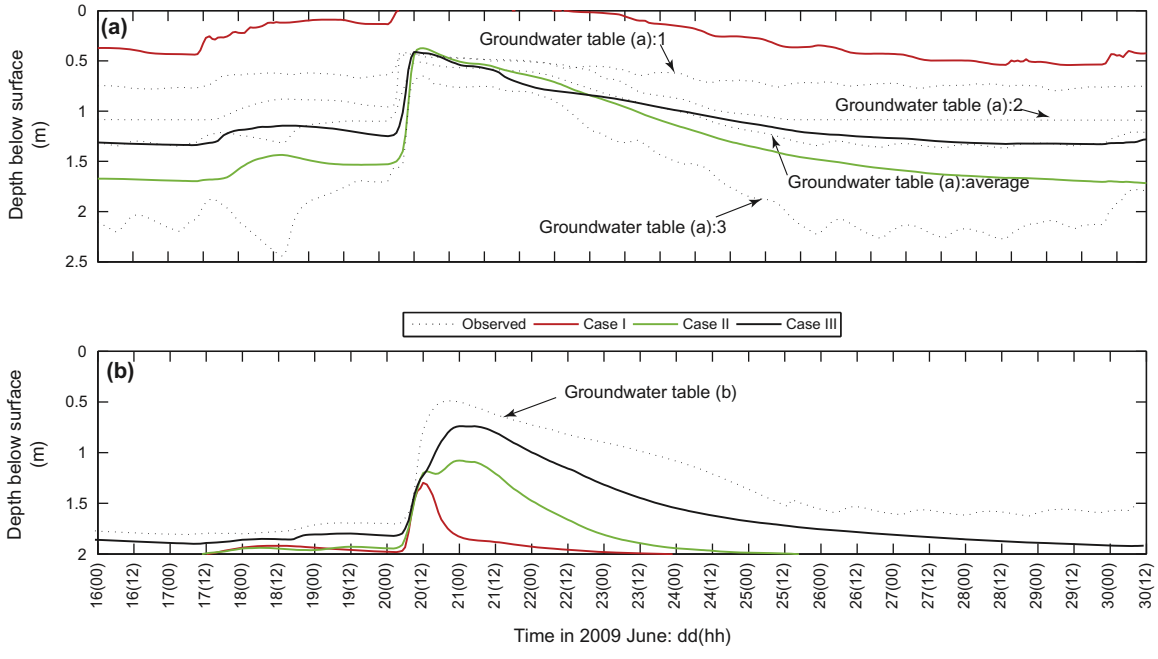

Fig. 5. Modeled shallow groundwater table at two specific locations in the catchment: (a) the triangle wells at the stream bank and (b) the well above the stream (see Fig. 1 for the specific locations).

differences in the responses of flow processes (Qu and Duffy, 2007). We argue that macropore effect at top layer within a threshold depth can satisfactorily represent the "fill and spill mechanism" of subsurface storm. We found that the matrix–macropore simplification for the subsurface flow can resolve the gap between soil database and hydrologic modeling applications. Our numerical simulations in Case I and Case II provide evidence that macropores are important to partitioning rainfall as subsurface or surface flow, which in turn is important to resolve the components of stormflow (Fig. 4). In the Cases II and III, we setup a threshold depth

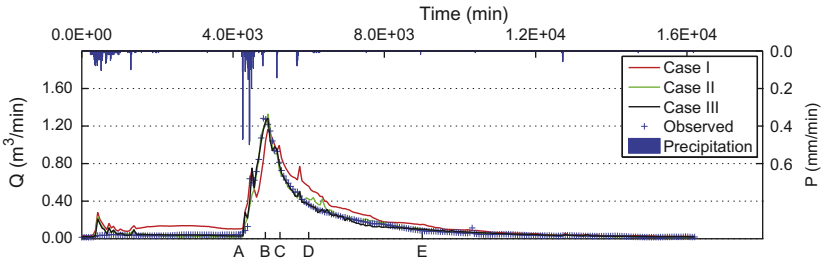

Fig. 6. Five timestamps are selected: A (pre-storm condition), B (peakflow reached), C (at the beginning of recession), D (in the middle of recession), and E (after recession).

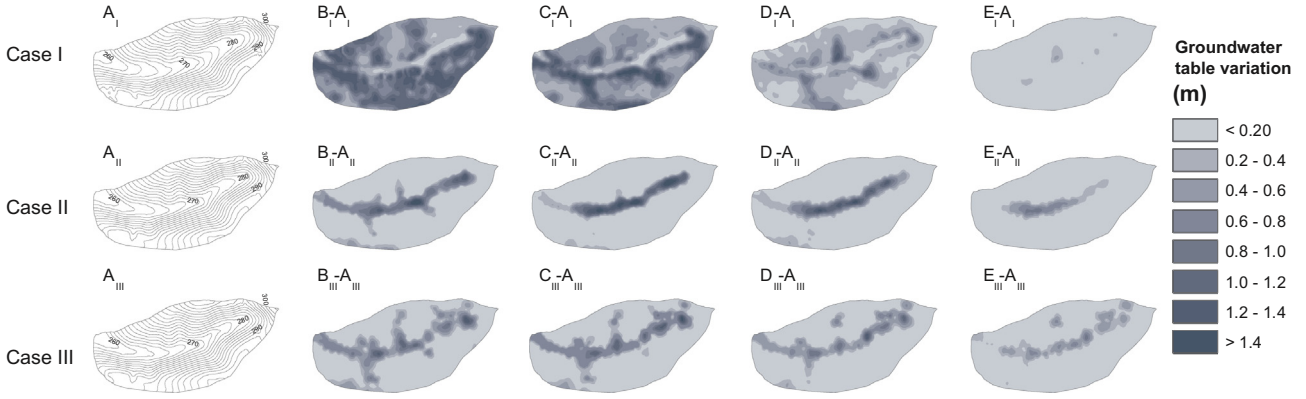

Fig. 7. Simulated spatial and response to a precipitation event for Cases I to III showing shallow groundwater table contours of pre-storm condition (column A), successive changes in saturated storage after precipitation event (B–A), (C–A), (D–A), (E–A).

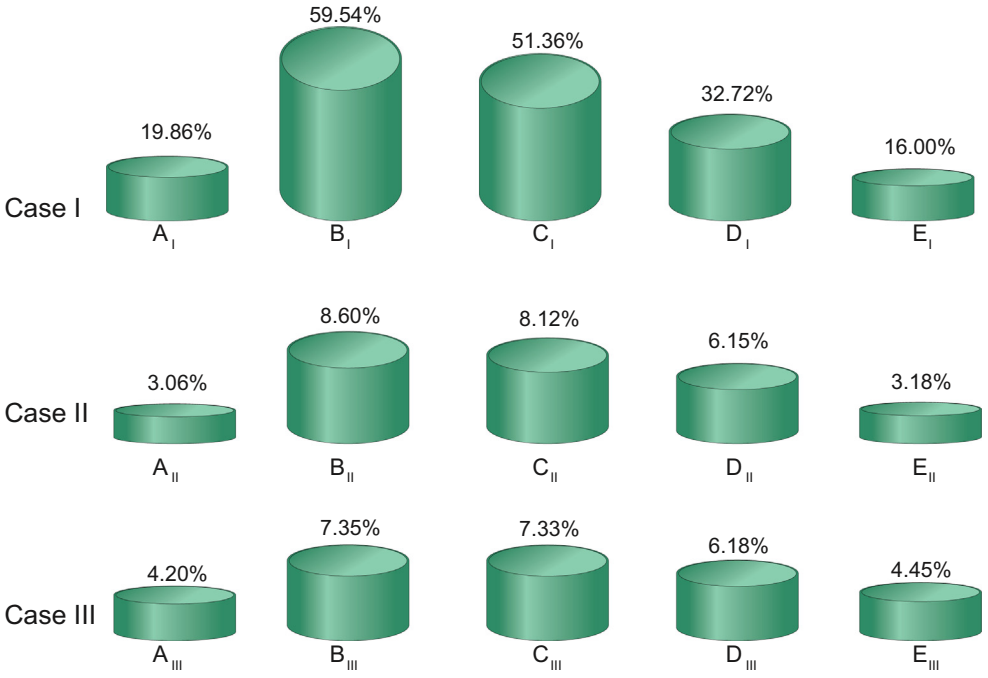

Fig. 8. The average percentage changes in saturated storage relative to the total pore volume during runoff event.

(macropore depth) for the calibration of macropore effects. The results suggested that threshold of macropore subsurface flow is around 2 m deep. Current soil survey data has huge gap for the description of macropore flow behavior. We argue that calibration is indispensible to estimate the combined hydraulic behavior of matrix and macropore in top layer soils, and vadose zone flow modeling parameterization resulted in variability of effective soil hydraulic parameters (Li et al., 2012).

The subsurface flow path in SSHCZO has been identified through field observations. Lin and Zhou (2008) concluded that the occurrence of subsurface preferential flow is very common in this watershed and it is controlled by intensity of rain, initial

moisture status, soil type, and landscape position. Our modeling studies resolved all these factors: we used high resolution (10-min) of meteorological forcing, fully coupled modeling between unsaturated–saturated layers, heterogeneous soil hydraulic properties and distributed domain representation. Graham and Lin (2011) argued that without lateral preferential flow routing, it would be difficult to model the moisture movement responses to precipitation. The modeling results also suggested the significant difference of lateral subsurface flow velocities when we added the macropore effect. Thomas et al. (2013) found that variation of isotopic composition was caused by lateral preferential flow. We argue that the field scale observations are difficult to generalize across the watershed. We anticipate that validating model results with distributed field data would be the future task for the comprehensive understanding of subsurface flow processes at SSHCZO.

4.2. What would be missed in the hydrologic modeling with coarse scale soil hydraulic properties?

Field scale soil hydraulic property measurements are one of the major supports of large-scale vadose zone modeling (Hopmans et al., 2002; Vereecken et al. 2008). Feddes et al. (1993) used a single set of effective soil hydraulic functions to represent for the whole watershed. A later study argued that effective soil parameters could well predict the area-averaged evaporation and subsurface runoff. Qu and Duffy (2007) explained the upslope ephemeral runoff responses with one set of soil hydraulic parameters. In the Case II of this study we also reproduced the stormflow in 2009 June. As noted by Grayson et al. (2002), environmental management not only require the quantity and quality of water in a stream, but also the spatial pattern across the watershed to rectify the problems such as hydrologic heterogeneity, contaminants sources, we compared the modeling predictions both along the streamflow and across the watershed. The similar internal runoff simulated in Cases II and III implied that limitation of streamflow as the single constraint in the parameter optimization of distributed hydrologic modeling (Grayson et al., 2002). We argue that the processes of calibration could resolve scale of soil hydraulic properties to enable satisfactory simulation results of an averaged watershed behavior (area-averaged evaporation, streamflow). The fine scale soil hydraulic properties are crucial to the scale-dependent processes, such as distributed water table dynamics and subsurface flow, which are important in the understanding of solute transport, biogeochemical processes (Andrews et al., 2011).

4.3. Calibrated parameters and field measurements

Usually, the hydrologic model calibration starts from soil hydraulic function data (from field measurements or databases) as a priori estimation of model parameters, and then nudges the parameters to obtain a set of effective parameters, which can optimally fit certain observed hydrologic variables. The meaning of these effective parameters and calibration processes have been always questioned and debated (Corwin et al., 2006; Dunn and Lilly, 2001; Grayson et al., 2002; Hopmans et al., 2002; Li et al., 2012; Vereecken et al., 2007). In this study, we started from the detailed field study results, and then employed the spatial pattern of soil hydraulic function to test the distributed hydrological modeling at SSHCZO. After calibration, the results suggested a gap between field measured soil hydraulic properties (Table 1) and PIHM model parameters (Table 4). Although both field-based soil hydraulic properties and calibrated parameters represented the spatial averaged effective values of each soil type, our understanding of the averaging processes in the model was limited, which was hardly consistent with field survey average. Another limitation was the understanding the variability of macropore conductivity. We noticed that the existence of macropore effect significantly improved the modeling ability in generation of subsurface stormflow. Field experiments results argued site-to-site variability, even vertical variability of soil hydraulic functions (Zhang et al., 2014). We claim the spatial heterogeneity at HFU level (Baldwin, 2011) is an appropriate scale for the catchment modeling. In addition, we anticipate an explicit link between modeling macropore flow and applicable field measurements in future studies.

5. Conclusions

This study assessed the effects of macropore and spatial variability of soil hydraulic properties using various soil survey dataset and the field measured soil parameters as inputs to distributed surface–subsurface flow simulations with the PIHM. Through distributed hydrologic modeling of the Shale Hills Catchment with different scales of soils datasets, the following conclusions are reached:

1. Soil water at top 2-m layer was highly influenced by macropore effect. Distributed modeling with macropore effect and lateral routing captured the quick responses of subsurface stormflow.
2. The spatial variability of soil hydraulic parameters is important in the modeling of distributed saturated storage dynamics and spatial pattern of subsurface flow.
3. The modeled results at the Shale Hills suggested that subsurface stormflow constituted a large part of the stream flow through the preferential flow pathways.

The findings from the study provide an important perspective on the resolution of soil hydraulic parameters. The delineated soil units of similar hydraulic characteristics based on the field monitoring data provide a meaningful parameterization scheme for distributed catchment modeling.

Acknowledgments

This research was funded by the Grant from the National Science Foundation, EAR 0725019 Shale Hills-Susquehanna Critical Zone Observatory and by the European Commission 7th Framework Programme as a Large Integrating Project (SoilTrEC, www.soiltrec.eu, Grant Agreement No. 244118). We would like to thank the reviewers of this manuscript for their constructive comments.

References

Alaoui, A., Caduff, U., Gerke, H.H., Weingartner, R., 2011. A preferential flow effects on infiltration and runoff in grassland and forest soils. Vadose Zone J. 10 (1), 367–377.

Anderson, S., Dietrich, W., Montgomery, D., Torres, R., Conrad, M., Loague, K., 1997. Subsurface flow paths in a steep, unchanneled catchment. Water Resour. Res. 33 (12), 1997.

Andrews, D.M., Lin, H., Zhu, Q., Jin, L., Brantley, S.L., 2011. Hot spots and hot moments of dissolved organic carbon export and soil organic carbon storage in the Shale Hills catchment. Vadose Zone J. 10 (3), 943–954.

Aubertin, G.M., 1971. Nature and extent of macropores in forest soils and their influence on subsurface water movement. USDA Forest Service Report, NE-192.

Baldwin, D., 2011. Catchment-scale Soil Water Retention Characteristics and Delineation of Hydropedological Functional Units in the Shale Hills Catchment, Pennsylvania State University.

Beven, K., Germann, P., 1982. Macropores and water flow in soils. Water Resour. Res. 18 (5), 1311–1325.

Beven, K., Germann, P., 2013. Macropores and water flow in soils revisited. Water Resour. Res. 49, 3071–3092.

Chen, F., Dudhia, J., 2001. Coupling an advanced land surface-hydrology model with the Penn State-NCAR MM5 modeling system. Part I: Model implementation and sensitivity. Mon. Weather Rev. 129 (4), 569–585.

Chen, C., Wagenet, R.J., 1992. Simulation of water and chemicals in macropore soils part 1. Representation of the equivalent macropore influence and its effect on soil–water flow. J. Hydrol. 130, 105–126.
Corwin, D.L., Hopmans, J., de Rooij, G.H., 2006. From field-to landscape-scale vadose zone processes: scale issues, modeling, and monitoring. Vadose Zone J. 5 (1), 129–139.
Dhillon, G.S., Inamdar, S., 2013. Storm event patterns of particulate organic carbon (POC) for large storms and differences with dissolved organic carbon (DOC). Biogeochemistry, 1–21.
Dingman, S.L., 2002. Physical Hydrology, second ed. Prentice Hall, New Jersey.
Duffy, C.J., Brandes, D., Shun, T.-Y., Sedmera, K., 2000. LDMS: A Low-Dimensional Modeling System for Hillslope, Catchment and River-Basin Runoff, US Army Research Office Report.
Dunn, S.M., Lilly, A., 2001. Investigating the relationship between a soils classification and the spatial parameters of a conceptual catchment-scale hydrological model. J. Hydrol. 252 (1), 157–173.
Dunne, T., 1978. In: Field Studies of Hillslope Flow Processes. John Wiley & Sons, Chichester, pp. 227–293.
Feddes, R.A., Menenti, M., Kabat, P., Bastiaanssen, W.G.M., 1993. Is large-scale inverse modelling of unsaturated flow with areal average evaporation and surface soil moisture as estimated from remote sensing feasible? J. Hydrol. 143 (1), 125–152.
Gerke, H.H., van Genuchten, M.Th., 1993. A dual-porosity model for simulating the preferential movement of water and solutes in structured porous media. Water Resour. Res. 29, 305–319.
Graham, C.B., Lin, H.S., 2011. Controls and frequency of preferential flow occurrence: a 175-event analysis. Vadose Zone J. 10, 816–831.
Grayson, R.B., Blöschl, G., Western, A.W., McMahon, T.A., 2002. Advances in the use of observed spatial patterns of catchment hydrological response. Adv. Water Resour. 25 (8), 1313–1334.
Hansen, N., 2011. The CMA Evolution Strategy: A Tutorial. <https://www.lri.fr/~hansen/cmatutorial.pdf>.
Hopmans, J.W., Nielsen, D.R., Bristow, K.L., 2002. How useful are small-scale soil hydraulic property measurements for large-scale vadose zone modeling? Geophys. Monogr. Ser. 129, 247–258.
Hopp, L., McDonnell, J.J., 2009. Connectivity at the hillslope scale: identifying interactions between storm size, bedrock permeability, slope angle and soil depth. J. Hydrol. 376 (3–4), 378–391.
Hutson, J.L., Wagenet, R.J., 1975. A multiregion model describing water flow and solute transport in heterogeneous soils. Soil Sci. Soc. Am. J. 59, 743–751.
Hwang, T., Band, L.E., Vose, J.M., Tague, C., 2012. Ecosystem processes at the watershed scale: hydrologic vegetation gradient as an indicator for lateral hydrologic connectivity of headwater catchments. Water Resour. Res. 48 (6).
Jin, L., Ravella, R., Ketchum, B., Bierman, P.R., Heaney, P., White, T., Brantley, S.L., 2010. Mineral weathering and elemental transport during hillslope evolution at the Susquehanna/Shale Hills Critical Zone Observatory. Geochim. Cosmochim. Acta 74 (13), 3669–3691.
Kabat, P., Hutjes, R.W.A., Feddes, R.A., 1997. The scaling characteristics of soil parameters: from plot scale heterogeneity to subgrid parameterization. J. Hydrol. 190 (3), 363–396.
Kumar, M., 2009. Toward a hydrologic modeling system. PhD Diss. The Pennsylvania State University, 251pp.
Kuntz, B.W., Rubin, S., Berkowitz, B., Singha, K., 2011. Quantifying solute transport at the shale hills critical zone observatory. Vadose Zone J. 10 (3), 843–857.
Lehmann, P., Hinz, C., McGrath, G., Tromp-van Meerveld, H.J., McDonnell, J.J., 2007. Rainfall threshold for hillslope outflow: an emergent property of flow pathway connectivity. Hydrol. Earth Syst. Sci. 11 (2), 1047–1063.
Li, R., Zhu, A., Song, X., Li, B., Pei, T., Qin, C., 2012. Effects of spatial aggregation of soil spatial information on watershed hydrological modelling. Hydrol. Process. 26 (9), 1390–1404.
Lin, H., 2006. Temporal stability of soil moisture spatial pattern and subsurface preferential flow pathways in the Shale Hills Catchment. Vadose Zone J. 5 (1), 317.
Lin, H., 2010. Linking principles of soil formation and flow regimes. J. Hydrol. 393 (1), 3–19.
Lin, H., Zhou, X., 2008. Evidence of subsurface preferential flow using soil hydrologic monitoring in the Shale Hills Catchment. Eur. J. Soil Sci. 59 (1), 34–49.
Lin, H.S., Kogelmann, W., Walker, C., Bruns, M.A., 2006. Soil moisture patterns in a forested catchment: a hydropedological perspective. Geoderma 131 (3), 345–368.
Lynch, J.A., 1976. Effects of antecedent soil moisture on storm hydrographs. Ph.D. Thesis. The Pennsylvania State University.
Lynch, J.A., Corbett, E.S., 1985. Source area variability during peakflow: a function of antecedent soil moisture content, in Watershed management in the eighties, ASCE.
McGuire, K.J., McDonnell, J.J., 2010. Hydrological connectivity of hillslopes and streams: characteristic time scales and nonlinearities. Water Resour. Res. 46 (10).
Meinzer, F.C., Woodruff, D.R., Eissenstat, D.M., Lin, H.S., Adams, T.S., McCulloh, K.A., 2013. Above-and belowground controls on water use by trees of different wood types in an eastern US deciduous forest. Tree Physiol. 33 (4), 345–356.
Mirus, B.B., Loague, K., 2013. How runoff begins (and ends): characterizing hydrologic response at the catchment scale. Water Resour. Res. 49 (5), 2987–3006.
Mirus, B.B., Ebel, B.A., Heppner, C.S., Loague, K., 2011. Assessing the detail needed to capture rainfall–runoff dynamics with physics-based hydrologic-response simulation. Water Resour. Res. 47, W00H10.
Mohanty, B.P., Bowman, S.R., Hendrickx, J.M.H., van Genuchten, M.T., 1997. New piecewise-continuous hydraulic functions for modeling preferential flow in an intermittent-flood-irrigated field. Water Resour. Res. 33, 2049–2073.
Mosley, M.P., 1982. Subsurface flow velocities through selected forest soils, South Island, New Zealand. J. Hydrol. 55 (1), 65–92.
Naithani, K.J., Baldwin, D.C., Gaines, K.P., Lin, H., Eissenstat, D.M., 2013. Spatial distribution of tree species governs the spatio-temporal interaction of leaf area index and soil moisture across a forested landscape. PLoS ONE 8 (3), e58704.
Qu, Y., Duffy, C.J., 2007. A semidiscrete finite volume formulation for multiprocess watershed simulation. Water Resour. Res. 43, W08419.
Rawls, W.J., Ahuja, L.R., Brakensiek, D.L., Shirmohammadi, A., 1993. Infiltration and soil water movement. In: Maidment, D.R. (Ed.), Handbook of Hydrology. McGraw-Hill Inc., New York (Chapter 5).
Shi, Y., Davis, K.J., Duffy, C.J., Yu, X., 2013. Development of a coupled land surface hydrologic model and evaluation at a critical zone observatory. J. Hydrometeorol. 14, 1401–1420.
Thomas, E.M., Lin, H., Duffy, C.J., Sullivan, P., Holmes, G.H., Brantley, S.L., Jin, L., 2013. Spatiotemporal patterns of water stable isotope compositions at the shale hills critical zone observatory: linkages to subsurface hydrologic processes. Vadose Zone J. 12 (4).
Tromp-van Meerveld, H.J., McDonnell, J.J., 2006a. Threshold relations in subsurface stormflow: 1. A 147-storm analysis of the Panola hillslope. Water Resour. Res. 42 (2).
Tromp-van Meerveld, H.J., McDonnell, J.J., 2006b. Threshold relations in subsurface stormflow: 2. The fill and spill hypothesis. Water Resour. Res. 42 (2).
Tromp-van Meerveld, H.J., Weiler, M., 2008. Hillslope dynamics modeled with increasing complexity. J. Hydrol. 361, 24–40.
Van Genuchten, M.T., 1980. A closed-form equation for predicting the hydraulic conductivity of unsaturated soils. Soil Sci. Soc. Am. J. 44 (5), 892–898.
van Schaik, N.L.M.B., Hendriks, R.F.A., van Dam, J.C., 2010. Parameterization of macropore flow using dye-tracer infiltration patterns in the SWAP model. Vadose Zone J. 9, 1–12.
VanderKwaak, J.E., 1999. Numerical simulation of flow and chemical transport in integrated surface–subsurface hydrologic systems. Doctorate Thesis. Department of Earth Sciences, University of Waterloo, Ontario, Canada.
Vereecken, H., Kasteel, R., Vanderborght, J., Harter, T., 2007. Upscaling hydraulic properties and soil water flow processes in heterogeneous soils. Vadose Zone J. 6 (1), 1–28.
Vereecken, H., Huisman, J.A., Bogena, H., Vanderborght, J., Vrugt, J.A., Hopmans, J.W., 2008. On the value of soil moisture measurements in vadose zone hydrology: a review. Water Resour. Res. 44 (4), 2008.
Vogel, T., Gerke, H.H., Zhang, R., Van Genuchten, M.T., 2000. Modeling flow and transport in a two-dimensional dual-permeability system with spatial variable hydraulic properties. J. Hydrol. 238, 78–89.
Vogel, T., Sanda, M., Dusek, J., Dohnal, M., Votrubova, J., 2010. Using oxygen-18 to study the role of preferential flow in the formation of hillslope runoff. Vadose Zone J. 9 (2), 252–259.
Watson, K.W., Luxmoore, R.J., 1986. Estimating macroporosity in a forest watershed by use of a tension infiltrometer. Soil Sci. Soc. Am. J. 50, 578–582.
Weiler, M., McDonnell, J., 2004. Virtual experiments: a new approach for improving process conceptualization in hillslope hydrology. J. Hydrol. 285 (1), 3–18.
Wösten, J.H.M., Pachepsky, Y.A., Rawls, W.J., 2001. Pedotransfer functions: bridging the gap between available basic soil data and missing soil hydraulic characteristics. J. Hydrol. 251 (3), 123–150.
Yu, X., Bhatt, G., Duffy, C., Shi, Y., 2013. Parameterization for distributed watershed modeling using national data and evolutionary algorithm. Comput. Geosci. 58, 80–90.
Zhang, J., 2011. Integrated approach to identifying subsurface flow in a forest catchment. Ph.D. Dissertation. The Pennsylvania State University.
Zhang, B., Tang, J.L., Gao, C., Zepp, H., 2011. Subsurface lateral flow from hillslope and its contribution to nitrate loading in streams through an agricultural catchment during subtropical rainstorm events. Hydrol. Earth Syst. Sci. 15 (10), 3153–3170.
Zhang, J., Lin, H., Doolittle, J., 2014. Soil layering and preferential flow impacts on seasonal changes of GPR signals in two contrasting soils. Geoderma 213, 560–569.